

Dynamics of bond-formation in some bound states of HeH^+

CH V RAMA RAO and ASISH K CHANDRA*

Department of Inorganic and Physical Chemistry, Indian Institute of Science,
Bangalore 560012, India

Abstract. The role of the electronic kinetic energy and its Cartesian components is examined during the formation of the ground ($^1\Sigma$), the first excited ($^1\Sigma$)* and the lowest ($^3\Sigma$) states of HeH^+ employing wavefunctions of the multi-configuration type with basis orbitals in elliptic coordinates. Results show, contrary to earlier beliefs, that the bond formation in these states is preceded primarily by a charge transfer from the neutral atom to the ion. There is no evidence of polarisation of the neutral atom orbitals by the ion even at large internuclear separation.

Keywords. Kinetic energy; bond-parallel and bond-perpendicular components; interference effect; charge transfer.

1. Introduction

The singly charged helium hydride molecular ion is known for many years from mass spectroscopic studies (Hogness and Lunn 1925). The ground state, ($^1\Sigma$), of HeH^+ dissociates into $\text{He} + \text{H}^+$ and is quite stable. The first excited ($^1\Sigma$)* and the lowest ($^3\Sigma$) states of HeH^+ dissociate into $\text{He}^+(^2S) (1s)$ and $\text{H}(^2S) (1s)$ with an exact energy of -2.5 Hartree. A good deal of discussion as to the nature of the first excited state of HeH^+ has appeared mainly because the exact shape of the potential curve is important in analysing the β -decay of the HT molecule as reported by Snell (1957) and Wexler (1959). These two excited states of HeH^+ are weakly bonding with an equilibrium separation of 5.5 Bohr for the first excited ($^1\Sigma$)* state and 4.5 Bohr for the lowest ($^3\Sigma$) state. Chemical bonding in these systems have been studied earlier by various authors (Coulson and Duncanson 1938; Hurley 1956; Anex 1963; Stuart and Matsen 1964; Peyerimhoff 1965; Politzer 1966; Michels 1966; Butscher and Schmidtke 1978). Classically the interaction between a polarisable atom and a singly charged particle produces an induced dipole in the atom and the energy change is given by

$$\Delta E = -\alpha/2R^4, \quad (1)$$

where α is the polarisability of the neutral atom and R is the internuclear separation. It had been shown by many authors (Stuart and Matsen 1964; Politzer 1966) that the polarisation interaction energies are quite close to the binding energies although an increasing discrepancy arises at small R values. The formation of the ground state ($^1\Sigma$) of HeH^+ was therefore viewed as resulting from polarisation of the He atom by H^+ , and that the exchange or interference effect was not important. Similarly the formation of the first excited ($^1\Sigma$)* and the lowest ($^3\Sigma$) states of HeH^+ was thought to arise from polarisation of the H-orbital by He^+ (Michels 1966). A previous study (Chandra and

Dedicated to Professor Sadhan Basu on the occasion of his 65th birth anniversary.
* To whom all correspondence should be addressed.

Sebastian 1976) on bond formation in terms of electronic forces also reveal that the origin of bonding in these two excited states is the ion-induced dipole type of interaction. However, our recent study (Rama Rao and Chandra 1985) of the formation process in terms of the bond-parallel and bond-perpendicular components of the kinetic energy show that polarisation is not important in the excited states.

In this paper we consider simple configuration interaction wavefunctions using orbitals in elliptic coordinates and then study the behaviour of the total electronic kinetic energy and its cartesian components as a function of R to reveal the dynamics of the bond-formation process in the ground, ($^1\Sigma$) and excited [$^1\Sigma^*$, ($^3\Sigma$)] states of HeH^+ . We then correlate our results derived from the kinetic energy to the change of densities that occurs during the formation process.

2. Computation of wavefunctions

We have chosen a simple configuration interaction wavefunction of the form

$$\Psi = \sum_i C_i \psi_i(\hat{r}), \quad (2)$$

where the spatial part $\psi_i(\hat{r})$ is given by

$$\psi_i(\hat{r}) = \phi_{1i}(1)\phi_{2i}(2) \pm \phi_{1i}(2)\phi_{2i}(1). \quad (3)$$

The plus and minus signs refer to the singlet and triplet states respectively. The orbitals $\phi_{ij}(\hat{r})$ are chosen to have the parametric form of the Harris type elliptic orbitals (Harris 1960)

$$\begin{aligned} \phi_{ji}(\hat{r}) = \exp[\delta_j \xi_j - \rho_j \eta_i] \xi_i^{n_j} \eta_i^{m_j} \exp(iv_j \phi_j) \\ \times [(\xi_i^2 - 1)(1 - \eta_i^2)]^{|v_j|/2} \end{aligned} \quad (4)$$

Where ξ_i, η_i and ϕ_i are the elliptical coordinates of the i th electron; δ_j, ρ_j, v_j , are the variables; n_j, m_j are the fixed parameters used for forming higher orbitals. The factor $\exp(iv_j \phi_j)$ determines the orbital angular momentum about the internuclear axis. The properties of these orbitals and evaluation of various integrals using these orbitals have been described by Harris (1960). Since the azimuthal correlation is small (Green *et al* 1974, 1978) and the error in the calculated kinetic energy arising from this is negligible (Rama Rao and Chandra 1985), we have chosen only three configurations ($v = 0$) for the description of the ground and the two excited states. Each configuration has four nonlinear parameters, $\delta_1, \rho_1, \delta_2$ and ρ_2 which are optimised at each value of R using the Powell-Botm algorithm (Kuester and Mize 1973). Results for the two excited states [i.e. ($^1\Sigma$)* and ($^3\Sigma$)] are discussed in a previous note (Rama Rao and Chandra 1985). Results for the ground state are as good as those published by Wolniewicz (1965). The wavefunctions of the ground and excited states are available from the authors on request.

3. Dynamics of bond formation in the ground state

In figure 1a is shown the total energy versus R for the ground state of HeH^+ . The classical polarisation energy is shown by the dashed lines where $\alpha \text{He} = 1.38 a_0^3$. If the

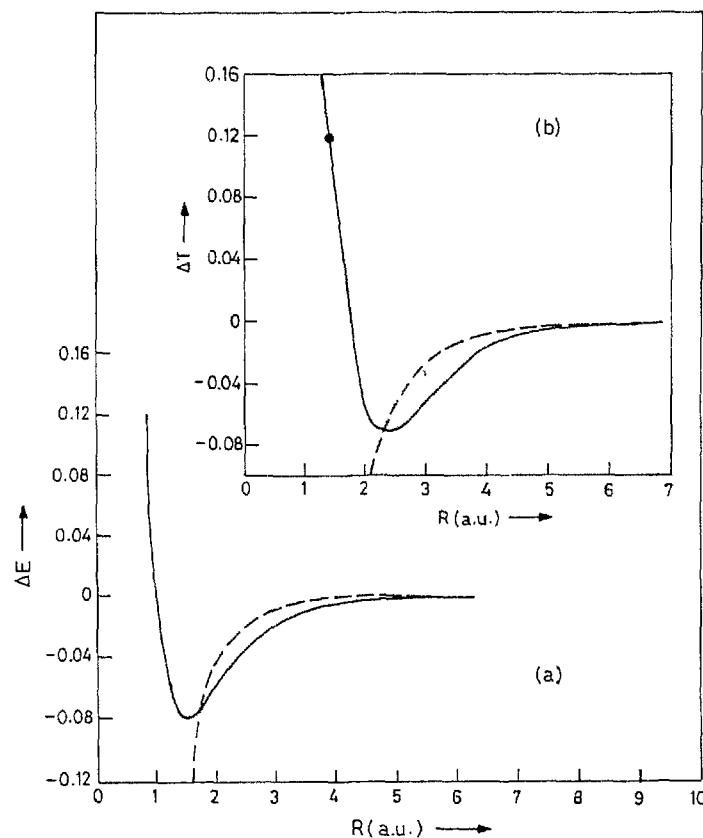


Figure 1. (a) Variation of ΔE with R for the lowest ($^1\Sigma$) state obtained from the *ab initio* wavefunctions. The dashed lines indicate the variation of the classical polarisation energy; (b) Variation of ΔT with R for the lowest ($^1\Sigma$) state. The dashed lines indicate the variation of ΔT according to (5). The black dot indicates the position of the equilibrium R .

variation of the total energy is due to this polarisation alone then by means of the virial theorem the kinetic energy change ΔT can be given by

$$\Delta T(R) = T(R) - T(\infty) = -(3\alpha/2R^4), \quad (5)$$

where $T(R)$ represents the expectation value of the kinetic energy of electrons at R . In figure 1b are shown the variations of ΔT with R , obtained from the *ab initio* wavefunctions of the ground state of HeH^+ , and by the dashed lines, the variation of ΔT according to (5). Both figures 1a and b reveal that at large R the polarisation interaction plays an essential role. The kinetic energy decreases because polarisation tends to expand the space occupied by electrons. As the atoms get closer, a volume exclusion process begins to occur (Matcha and King 1977). Electrons tend to occupy a smaller volume, the uncertainty in the position of electrons decreases and the kinetic energy increases. Therefore, formation of HeH^+ can be viewed, in essentially classical terms, as resulting from polarisation of He by H^+ . This was also the conclusion of Politzer (1966) who believed that the exchange factor (or resonance) is unimportant as this would require overcoming the high ionisation potential of helium.

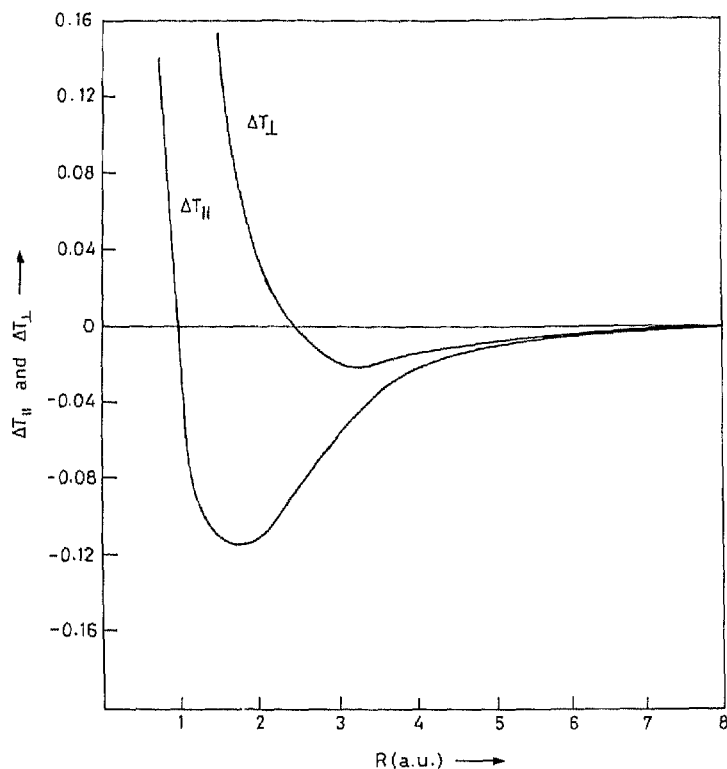


Figure 2. Variations of $\Delta T_{||}$ and ΔT_{\perp} with R for the lowest (${}^1\Sigma$) state of HeH^+ .

We then consider the geometric partitioning of T as $T_{||}$ (bond-parallel) and T_{\perp} (bond-perpendicular) components. In figure 2 is shown the variation, with R , of $\Delta T_{||}(R)$ [i.e. $T_{||}(R) - T_{||}(\infty)$] and $\Delta T_{\perp}(R)$ [i.e. $T_{\perp}(R) - T_{\perp}(\infty)$] for the ground state. The $T_{||}(\infty)$ and $T_{\perp}(\infty)$ are taken as $1/3$ and $2/3$ times respectively, the atomic kinetic energy term. If $\Delta T(R)$ be given by (5) then one expects for the polarisation effect alone

$$\Delta T_{||}(R) = 1/2 \Delta T_{\perp}(R) = -(\alpha/2R^4). \quad (6)$$

Figure 2 shows, however, that the magnitude of $\Delta T_{||}(R)$ at large R is larger than $\Delta T_{\perp}(R)$, contrary to the expectations from (6). ΔT_{\perp} decreases initially very slowly and then increases rather rapidly while $\Delta T_{||}$ continues to decrease until $R = 1.8$ au, when it begins to increase. According to Ruedenberg's analysis (Ruedenberg 1975; Feinberg and Ruedenberg 1971) of H_2^+ , this increase of T_{\perp} and decrease of $T_{||}$ as the atoms get closer to each other arise from the interference effect.

The interference effect in HeH^+ can arise from the charge transfer from the neutral He atom to H^+ in the following way. We consider the following approximate wavefunction of HeH^+

$$\Psi = [a(1) a(2) + \lambda a(1) b(2)] / [1 + \lambda^2 + 2\lambda \langle a|b \rangle]^{1/2} \quad (7)$$

where

$$\lambda = 0 \text{ for } R = \infty; \lambda > 0 \text{ for } R < \infty, \quad (8)$$

and 'a' and 'b' are the Slater type 1s orbitals of He and H, respectively. Using wavefunction (7), one obtains

$$\langle T \rangle = [2T_a + \lambda^2(T_a + T_b) + 2\lambda(T_a \langle a|b \rangle + \langle a|\hat{T}|b \rangle)]/[1 + \lambda^2 + 2\lambda \langle a|b \rangle] \quad (9)$$

$$\Delta T = \langle T \rangle - T_{\text{He}} \approx 2\lambda[\langle a|\hat{T}|b \rangle - T_a \langle a|b \rangle], \quad (10)$$

where $T_a = 1.44$ au, since $\Delta T = \Delta T_{\parallel} + \Delta T_{\perp}$ one can write:

$$\Delta T_{\parallel}(R) \approx 2\lambda[\langle a|\hat{T}_{\parallel}|b \rangle - 0.48 \langle a|b \rangle], \quad (11)$$

$$\Delta T_{\perp}(R) \approx 2\lambda[\langle a|\hat{T}_{\perp}|b \rangle - 0.96 \langle a|b \rangle]. \quad (12)$$

These two-centre kinetic energy integrals involving 1s orbitals are discussed by Ruedenberg (Feinberg and Ruedenberg 1971; Ruedenberg 1975) and also by Baumann and Heilbronner (1966). They have shown that at large R , $\langle a|\hat{T}_{\parallel}|b \rangle$ decreases and $\langle a|\hat{T}_{\perp}|b \rangle$ increases with decreasing R . Equations (11) and (12) can qualitatively explain the large initial decrease of ΔT_{\parallel} while the initial increase of ΔT_{\perp} is cancelled by the second term of (12). This analysis therefore suggests that the bond-formation in the lowest (¹Σ) state of HeH⁺ arises from the interference effect following the flow of charge from He to H⁺. The bond-formation is not preceded by the classical polarisation of He by H⁺. This is not surprising as the polarisability of He is very small. Politzer (1966) argued that the charge-transfer from He to H⁺ is difficult as the ionisation potential of He is high. But when a positive ion approaches a neutral atom the high ionisation potential of the neutral atom can be overcome by the attractive energy of the electron with the approaching positive ion (i.e. $-e^2/R$).

4. Electron densities on the atoms in HeH⁺ (¹Σ)

Butscher and Schmidtke (1978) partitioned the total molecular electron density into quasi classical, q^c and interference, q^i terms. When the interference term is integrated over all space, it gives zero, while q^c of the atom gives the number of electrons in the atom. They found that for the nearly dissociated system ($R = 10$ au), $q(\text{He}) = 1.9999$ and $q(\text{H}) = 0.0001$ (see table 3 of Butscher and Schmidt 1978). This result indicates that even at large R , charge migration has taken place. They have used Slater-type orbitals on each atomic centre. It is not possible with elliptic orbitals to partition the total density into the quasi-classical and interference terms. We have calculated the density on the H and He nuclei in HeH⁺ as a function of R . They are denoted by $\rho_{\text{H}}(R)$ and $\rho_{\text{He}}(R)$ in figures 3a and b. In the same figure (3a) the density of the He atom, q_{He} as a function of R from the nuclear centre is shown. These densities are obtained from the wavefunction of the He atom given by Silverman *et al* (1960). Figures 3a and b, show that the density on the H-nucleus is always greater than that expected from the classical penetration of a proton into the undeformed charge cloud of He. On the other hand, figure 3b shows that as R is decreased, the density on the He nucleus decreases. These results corroborate our findings from kinetic energy studies that charge-transfer from He to H⁺ takes place before the bond is formed. But these results do not completely rule out the possibility of polarisation of He by H⁺. As the He atom is polarised, density on the He nucleus should decrease while the tail of the He atom wavefunction should increase toward the proton causing a raise in density on the proton centre. It should be

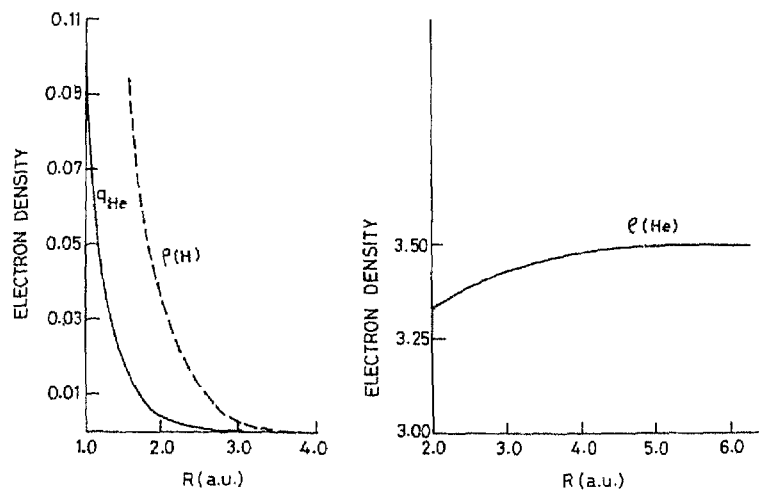


Figure 3. The variation of $\rho(\text{H})$ and $\rho(\text{He})$ in the lowest ($^1\Sigma$) state of HeH^+ with R . The variation of the free atom density of He, q_{He} with R from the nuclear centre is also shown.

noted that the analysis of the T_{\parallel} and T_{\perp} components (figure 2) can unequivocally reveal that bonding in HeH^+ is not preceded by polarisation.

5. Dynamics of bond-formation in the first excited, i.e., ($^1\Sigma$)* and the lowest ($^3\Sigma$) states of HeH^+

Our *ab initio* calculations on these two states of HeH^+ show that both dissociate into He^+ and H and exhibit weak bonding. Our calculations further reveal that the ($^3\Sigma$) state is about 2.3 times more stable than the ($^1\Sigma$)* state. In figure 4 are shown the variations of $\Delta T(R)$ with R calculated from the *ab initio* wavefunctions of the ($^1\Sigma$)* and ($^3\Sigma$) states. At large R , the H-orbital is expected to be polarised by He^+ and $\Delta T(R)$ obtained from the classical polarisation is shown in the same figure by the dashed lines. The polarisability α of the H atom is $4.5 a_0^3$. At large R , the kinetic energy change is the primary contributor to the long-range attractions. If bond formation in the ($^1\Sigma$)* and ($^3\Sigma$) states of HeH^+ is preceded by polarisation then in the initial stage kinetic energy should decrease as shown in figure 4 because polarisation tends to expand the space where the electrons move. Figure 4 gives therefore an impression that the weak bonding in these two states of HeH^+ is due to ion-induced dipole attraction. Since bond energies of these weakly bound states are in the range of 1–2 kcal/mol and the polarisation energy is also of the same order near $R \sim 5.0$ Bohr, such inference has not been called into question.

We then consider T_{\parallel} and T_{\perp} . In figure 5 are shown the variations with R of ΔT_{\parallel} and ΔT_{\perp} for the ($^1\Sigma$)* and ($^3\Sigma$) states. Figure 5 shows again that ΔT_{\perp} slowly increases from zero while ΔT_{\parallel} decreases. Thus the bond formation in these two states is not preceded by polarisation. Our recent analysis (Rama Rao and Chandra 1985) based on the kinetic energy components reveals that bond formation in these two states is preceded by charge-transfer from the $1s$ orbital of H to the $2s$ orbital of He^+ . Since the energy of the $^3S(1s\ 2s)$ state is lower than that of $^1S(1s\ 2s)$ state of He, a greater amount

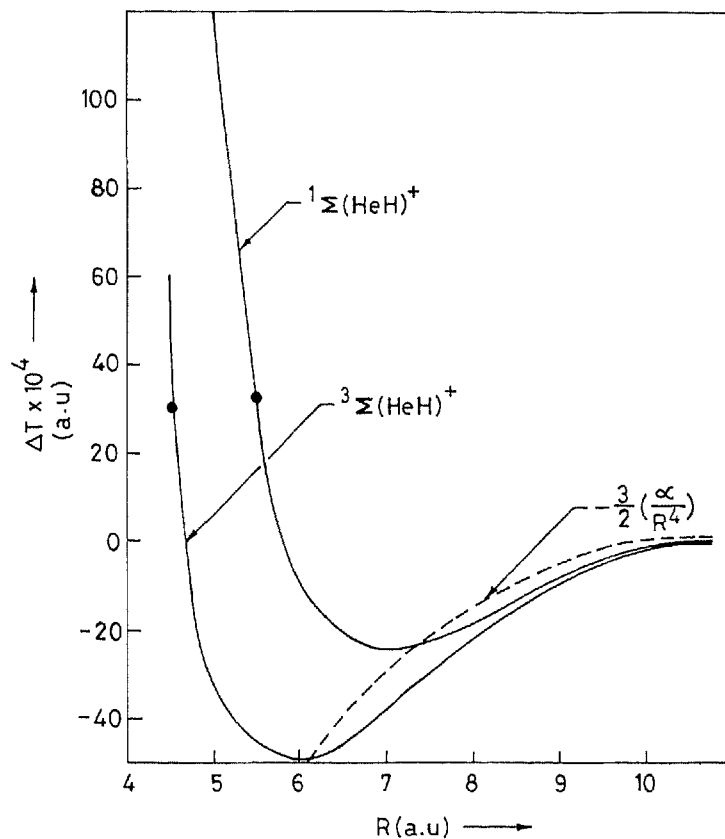


Figure 4. Variation with R , of ΔT for the first excited ($1\Sigma^*$) and the lowest (3Σ) states of HeH^+ . The dashed lines indicate the variation of ΔT obtained from classical polarisation.

of charge-transfer and hence a larger initial lowering of ΔT (and ΔT_{\parallel}) is expected for the (3Σ) state. Thus the difference in bonding in these two excited states of HeH^+ arises from the different extent of charge-transfer from H to He^+ .

6. The density and density difference maps of HeH^+ in its first excited ($1\Sigma^*$) and lowest (3Σ) states

Roux *et al* (1956) had earlier introduced the definition of the charge density difference function as

$$\Delta\rho(\hat{r}) = \rho_m(\hat{r}) - \rho_a(\hat{r}) \quad (13)$$

as the difference in the distribution of electronic charge density between that found in the molecule, $\rho_m(\hat{r})$ and that obtained by the superposition of the unperturbed atomic densities $\rho_a(\hat{r})$. The $\rho_a(\hat{r})$ is expressed as a sum of the contributions from each of the separated atom densities, the nucleus of each atom occupying a position identical to that found in the molecular system. Contour maps of $\rho_m(\hat{r})$ and $\Delta\rho(\hat{r})$ display the densities

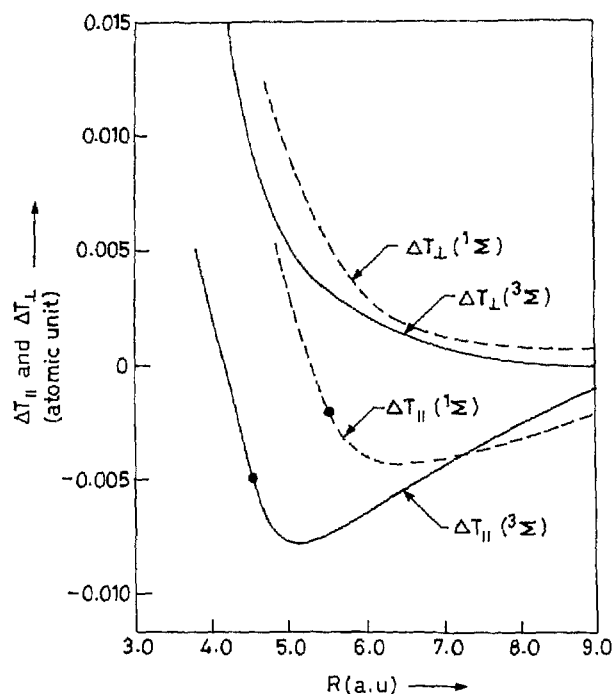


Figure 5. Variation of $\Delta T_{||}$ and ΔT_{\perp} with R for the first excited ($^1\Sigma$)* and lowest ($^3\Sigma$) of HeH^+ .

and the change of densities that occur during the formation of molecules.

The total molecular density distributions $\rho_m^{(p)}$ for the ($^1\Sigma$)* ($R_e = 5.5$ Bohr) ($^3\Sigma$) ($R_e = 4.5$ Bohr) states of HeH^+ are shown in figure 6. The first contour envelop both the nuclei in HeH^+ has a value less than or equal to 0.005. A contours of higher density are closed separately around each nucleus. Thus the portion of the total electron density is centred on the nuclei in both the states. The very different from the ρ_m -map of the ($^1\Sigma_g^+$) state of H_2 (Wahl 1966) where even contours of values larger than 0.01 encompass both the nuclei at R_e indicating a sharing of electrons.

In figure 7 are shown $\Delta\rho$ -maps for the ($^1\Sigma$)* and ($^3\Sigma$) states of HeH^+ at the individual values of R . Figure 7 shows the deformation of density around the H-nucleus to the He nucleus. This deformation could arise from polarisation of the H-atom by or by charge transfer from H to He^+ . The negative $\Delta\rho$ region behind the H-nucleus indicative of charge transferred from behind the H-nucleus. As R is decreased, there is no indication of a single contour line of positive $\Delta\rho$ enveloping both nuclei corresponding to a shared density as in H_2 (Bader and Chandra 1968). In both the ($^1\Sigma$)* and ($^3\Sigma$) states, the distribution of charge transferred from hydrogen is accumulated on the H-side of the internuclear region. This leads to unsymmetrical distribution of charge in the internuclear region. The charge build-up in the internuclear region in the first excited ($^1\Sigma$)* and the lowest ($^3\Sigma$) states does not therefore arise from the same of electron sharing observed in H_2 . This unsymmetrical charge distribution can be understood more easily in terms of Slater type orbitals. When the 1s orbitals of

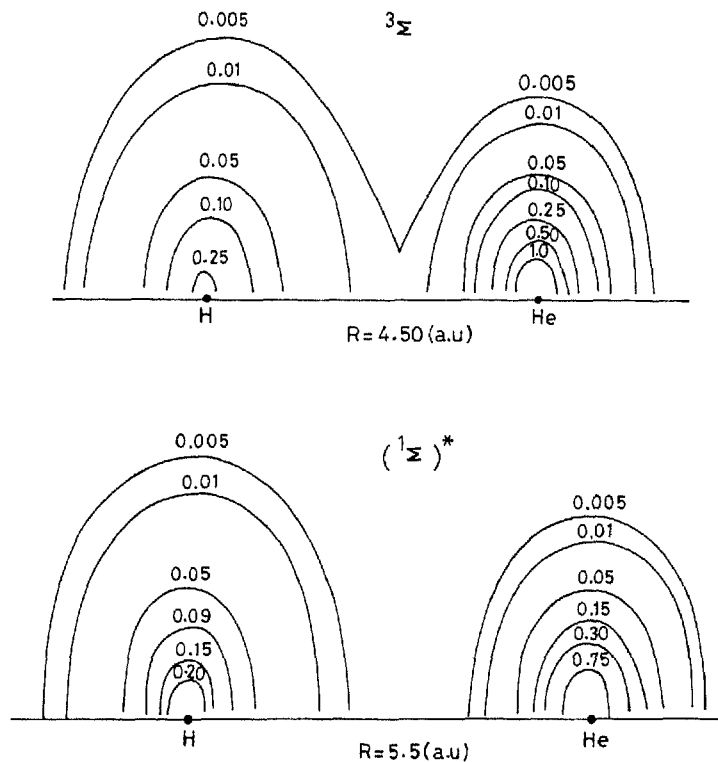


Figure 6. Density contour maps for the $(^1\Sigma)^*$ and $(^3\Sigma)$ states at their respective R_e values.

and H are brought closer, electrons cannot exchange as in H_2 because these two orbitals differ in energy by 40 eV. Since the $2s$ orbital of He^+ is degenerate with the $1s$ orbital of H, on closer approach the electron of H can move to the $2s$ orbital of He^+ . This $1s$ - $2s$ overlap leads to unsymmetrical charge distribution in the internuclear region and is also responsible for the observation of interference effect at larger R .

Any distribution of charge in a chemical bond must account for the electrostatic stability. Since the charge is heavily concentrated on the proton side of the internuclear region, the force exerted on the He nucleus by this density is so great that the He nucleus can reach electrostatic equilibrium only by having its own density polarised away from the H atom. This is the origin of the negative $\Delta\rho$ near the He nucleus in the internuclear region.

7. Conclusions

We may, therefore, conclude that in both the ground and excited states of HeH^+ the polarisation of the neutral atom orbitals by the positive ion is not important even at large R , contrary to earlier beliefs. Bond formation in these states is preceded by charge-transfer from the neutral atom to the positive ion. The interference effect following the charge-flow from one centre to another causes bonding. It should also be noted that an

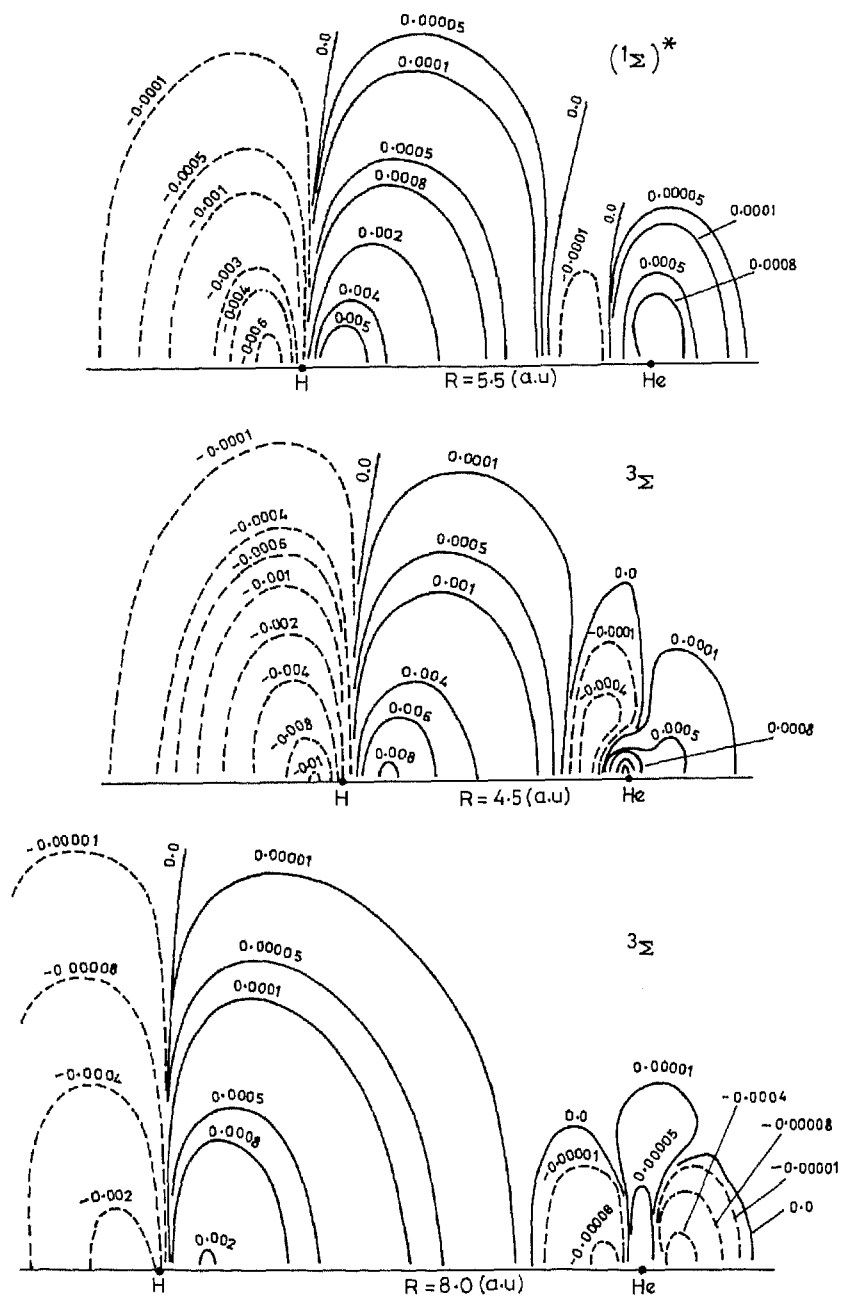


Figure 7. Density difference i.e. $\Delta\rho$ -maps of the $(1\Sigma)^*$ and (3Σ) states at the indicated values of R .

Analysis based on the variation of the total energy or total kinetic energy with R may give rise to misleading information about the dynamics of the bond formation process.

Acknowledgement

One of us (CH V R R) thanks the Department of Atomic Energy for financial support.

References

- Alex B G 1963 *J. Chem. Phys.* **38** 1651
 Anderson R F W and Chandra A K 1968 *Can. J. Chem.* **46** 953
 Baumann H and Heilbronner E 1966 *Theor. Chim. Acta* **6** 95
 Bartscher W and Schmidtke H 1978 *Chem. Phys.* **30** 41
 Chandra A K and Sebastian K L 1976 *Mol. Phys.* **31** 1489
 Coulson C A and Duncanson W F 1938 *Proc. R. Soc. London* **A165** 90
 Dettl A A 1956 *J. Chem. Phys.* **24** 150
 Einfeld M J and Ruedenberg K 1971a *J. Chem. Phys.* **54** 1495
 Einfeld M J and Ruedenberg K 1971b *J. Chem. Phys.* **55** 5804
 Goudisman J 1965 *J. Chem. Phys.* **43** 3037
 Green T A, Michels H H and Browne J C 1974 *J. Chem. Phys.* **61** 5186
 Green T A, Michels H H, Browne J C and Madson M M 1978 *J. Chem. Phys.* **69** 101
 Harris F E 1960 *J. Chem. Phys.* **32** 3
 Huggins T R and Lunn E C 1925 *Phys. Rev.* **26** 44
 Hurley A C 1956 *Proc. Phys. Soc.* **A69** 868
 Lester J J and Mize J H 1973 *Optimisation techniques with FORTRAN* (New York: McGraw Hill)
 Maitra R and King S C 1977 *J. Chem. Phys.* **66** 5786
 Michels H H 1966 *J. Chem. Phys.* **44** 3834
 Meyerimhoff S 1965 *J. Chem. Phys.* **43** 998
 Mitter P 1966 *J. Chem. Phys.* **45** 1856
 Prasad Rao CH V and Chandra A K 1985 *Chem. Phys. Lett.* **113** 391
 Raux M, Besnainon S and Daudel R 1956 *J. Chem. Phys.* **54** 218
 Ruedenberg K 1975 in *Localisation and delocalisation in quantum chemistry* (eds O Chavet, R Daudel, S Diner and J P Malrieu (Dordrecht: D Reidel) vol. 1
 Sverman J N, Platas O and Matsen F A 1960 *J. Chem. Phys.* **32** 1402
 Seil A H 1957 *J. Inorg. Nucl. Chem.* **5** 112
 Smart J D and Matsen F A 1964 *J. Chem. Phys.* **41** 1646
 Stahl A C 1966 *Science* **151** 961
 Szklar S 1959 *J. Inorg. Nucl. Chem.* **10** 8
 Szyniewicz L 1965 *J. Chem. Phys.* **43** 1087